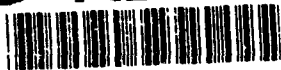AD-A257 852

REGIONAL WAVE ATTENUATION IN EURASIA

Kin-Yip Chun
Tianfei Zhu
Xiao Rung Shih

University of Toronto
Department of Physics
60 St George Street
Toronto, Ontario
M5S 1A7, Canada

DTIC
S ELECTE **D**
NOV 2 3 1992
A

October 1992

Scientific Report Number 2
27 September 1991 - 27 September 1992

30 p4

92

7

REPORT DOCUMENTATION PAGE

Public reporting burden for this collection of information is estimated to average 1 hour per response, including the time for reviewing instructions, searching existing data sources, gathering and maintaining the data needed, and completing and reviewing the collection of information. Send comments regarding this burden estimate or any other aspect of this collection of information, including suggestions for reducing this burden, to Washington Headquarters Services, Directorate for Information Operations and Reports, 1215 Jefferson Davis Highway, Suite 1204, Arlington, VA 22202-4302, and to the Office of Management and Budget, Paperwork Reduction Project (0704-0188), Washington, DC 20503.

1. AGENCY USE ONLY (Leave blank)	2. REPORT DATE October 1992	3. REPORT TYPE AND DATES COVERED Annual Tech Rep 9/27/91-9/30/92

4. TITLE AND SUBTITLE	5. FUNDING NUMBERS
REGIONAL WAVE ATTENUATION IN EURASIA	
6. AUTHOR(S) Kin-Yip Chun Tienfei Zhu Xiao Rung Shih	F29601-91-C-DB24

7. PERFORMING ORGANIZATION NAME(S) AND ADDRESS(ES)	8. PERFORMING ORGANIZATION REPORT NUMBER
Geophysics Division, Department of Physics University of Toronto, 60 St. George Street Toronto, Ontario M5S 1A7 Canada	NA

9. SPONSORING/MONITORING AGENCY NAME(S) AND ADDRESS(ES)	10. SPONSORING/MONITORING AGENCY REPORT NUMBER
DARPA/NMRO, 3701 North Fairfax Drive, Arlinton, VA 22203-1714 Contracting Officer Representative: Dr. Alan S. Ryall	NA

11. SUPPLEMENTARY NOTES

12a. DISTRIBUTION/AVAILABILITY STATEMENT	12b. DISTRIBUTION CODE
APPROVED FOR PUBLIC RELEASE DISTRIBUTION UNLIMITED	

13. ABSTRACT (Maximum 200 words)

Presented in the Scientific Report Number 2 are our research efforts in the first year of our two-year project in regional wave studies in Eurasia. Based on the reversed two-station method (RTSM), our research has led to development in methodology, i.e., formulation of the source pair/receiver pair (SPRP) method and the extended RTSM, suitable for attenuation study using data from sparsely-located stations. These methods are more flexible in making use of the regional data from Eurasia. Compared to the RTSM, results from either method lead to measurements of the frequency-dependent anelastic attenuation in an area instead of inter-station (event) paths. Application of the SPRP method to the CDSN/IRIS data from regional and far-regional distances has shown that L_g attenuation at low frequencies (0.1-1.0 Hz) exhibits greater stability and consistency than its higher-frequency counterpart. Application of the extended RTSM to the local and regional recordings from Beijing Telemetered Network (BTN) has shown that the area under BTN is characterized by relatively high L_g attenuation, compared to the non-Tibetan portion of the Eurasian continent.

14. SUBJECT TERMS			15. NUMBER OF PAGES
Lg ATTENUATION EURASIA IRIS CDSN BTN TIME-DOMAIN ANALYSIS REGIONALIZATION			16. PRICE CODE

17. SECURITY CLASSIFICATION OF REPORT	18. SECURITY CLASSIFICATION OF THIS PAGE	19. SECURITY CLASSIFICATION OF ABSTRACT	20. LIMITATION OF ABSTRACT
Unclassified	Unclassified	Unclassified	SAR

TABLE OF CONTENTS

DTIC QUALITY INSPECTED

Accesion For		
NTIS CRA&I		☑
DTIC TAB		☐
Unannounced		☐
Justification		
By		
Distribution /		
Availability Codes		
Dist	Avail and/or Special	
A-1		

I. INTRODUCTION

1.1 Background

Over the years the DARPA research program to develop regional discrimination procedures has produced numerous advances in our understanding of the regional phases generated by seismic sources. The installation of the IRIS/CDSN stations in the former Soviet Union and the People's Republic of China and well-managed data transition from these stations to the Center of Seismic Studies (CSS) have provided opportunities to study regional wave propagation in Eurasia with high-quality three-component recordings. These have brought advances in understanding the characteristics of the wave propagation and source discrimination in the region as evidenced by the 14th PL/DARPA Annual Meeting. The objective of our program under DARPA funding is to obtain frequency-dependent P_n and L_g attenuation measurements that are accurate enough to result in significant improvement in seismic monitoring in nuclear verification. Scientifically, our research intends to investigate the frequency-dependent attenuation of the regional phases in Central Asia, especially in China, where the aspect has never been studied. Technically, we emphasize developments in methodology to isolate frequency-dependent, non-propagating contaminants (geological site effects, instrument response error, etc.) from seismic wave propagation effects (geometrical spreading and attenuation).

To fulfill the above objectives, we have transcribed and processed data from two databases, i.e., three-component broadband data from the IRIS/CDSN stations in Eurasia and single-component data from the Beijing Telemetered Network (BTN). Although data from the IRIS and CDSN stations may contain information of wave propagation under a very large region, an intrinsic difference between the two recording systems is that the CDSN stations were set to triggered mode while the IRIS stations record continuously. We have transcribed data from events with magnitude greater than 5 (mb) so that for a single event, there are reasonable number of good S/N records from both CDSN and IRIS stations. By the end of the first year, we have developed procedures, which are capable of providing consistent site/source corrected attenuation measurements with data collected by sparsely located broadband stations in Eurasia. To study frequency-dependent attenuation in Eurasia, data from the BTN appears to be an important component as the network records seismicity at local and regional distance ranges from neighboring regions of active tectonics. In contrast to the distribution of the broadband stations in Eurasia, recordings from the relatively dense array of the BTN provide opportunities to test and develop procedures with different geometric considerations, and to compare with the existing methods, which have been successfully applied elsewhere.

1.2 Research on Methodology of Regional Wave Attenuation

Chun et al. (1987) have shown that by using reversed two-station method (RTSM), L_g attenuation along short Canadian Shield (high-Q) paths can be accurately measured in the presence of strong site effects and unknown instrument response errors. The method was extended, with a least-squares inversion scheme, to obtain the frequency dependence of both geometrical

spreading (n) and anelastic attenuation (γ) for P_n wave propagation in Eastern Canada (Zhu et al., 1991). Central to our project is to develop a generalized method for the regional wave attenuation study in Eurasia, based on the procedures that were successfully applied in Eastern Canada. The development in methodology considered here emphasizes the application suitable for data from sparsely-located network stations.

Two methods have been formulated and tested during the first year of our project, i.e., source pair/receiver pair method (SPRP) and the extended reversed two station method (extended RTSM). Compared to the RTSM, the geometric restriction on the input ray paths to the SPRP method is relaxed in the situation where there are not enough collinear station-event pairs, i.e., ray paths from the seismic events to stations along the great-circle paths. When the effect of the source radiation pattern is considered minor as in the case of L_g wave propagation, relaxation of the geometric restriction increases the number of station-event pairs and therefore, leads to statistically stable results. However, the effect of the source radiation pattern cannot be entirely neglected as in the case of P_n or S_n wave propagation. Hence, we have developed the extended RTSM, the first step of which requires ray paths between the two stations and one event be collinear to cancel the source effect. To accommodate the situation where the collinear reversal does not exist, the extended RTSM employs a triangular configuration, which cancels the site effect by combining three station-event pairs. Further, the formulation of the two methods has shown that with slight difference in computer programming, we can carry out the simultaneous site and source correction regardless the stations straddle the events or vice versa. The report provides a description of each method and its application in the L_g wave attenuation studies.

1.3 Organization of the Report

This report is divided into four sections including this introduction. Section II comprises a brief derivation of the SPRP method and its time-domain application to the L_g wave attenuation study in Eurasia. Earthquakes of regional and far-regional distances are used in this analysis. Previous studies in the region have mostly employed techniques in the frequency domain. We present it in time domain because (1) the result is directly applicable to the source scaling and discrimination, and (2) at the distance range from a few hundreds to five thousands kilometers, we found in the same data set the results from the time-domain analysis is superior than those in frequency domain as shown previously by Chun et al. (1992). Section III comprises a brief derivation of the extended RTSM, and its application to the L_g wave attenuation study in data from BTN. Preliminary results from the frequency-domain analysis show that attenuation in the area under BTN is relatively high. The analysis has also revealed that large discrepancies may exist between the time- and frequency-domain results. Finally, Section IV provides a summary of our research effort in the first year and identifies the future plans.

II. TIME-DOMAIN ANALYSIS OF L_g WAVE ATTENUATION IN EURASIA

2.1 Introduction

Knowledge of regional wave attenuation, especially that of the L_g waves, is prerequisite to reliable seismic source parameter retrieval. While seismic attenuation studies have been numerous over the past two decades, most published results pertain to frequency-domain measurements which have paid little attention to the time-resolution or waveform features of the regional signatures being studied. It is thus interesting to observe that modern waveform (time-domain) analysis frequently requires attenuation corrections to be applied to a short, specific portion of a seismic record, as exemplified by Nuttli's method (Nuttli, 1986, and 1988) of explosion yield estimation using L_g waves. It appears that attenuation estimates derived from a dominant part of an L_g wavetrain could be more useful in seismic verification than frequency-domain estimates derived from arbitrarily selected time or group velocity windows, which are typically much longer than the dominant portion of L_g wavetrains.

The current research project seeks to remedy the apparent shortcomings of the frequency-domain attenuation measurement techniques while retaining the unique capability of the RTSM method for simultaneous corrections of source and site effects (Chun et al., 1987). The new technique, termed SPRP (Chun and Zhu, 1992), is tested on Eurasian seismic data for its performance and suitability as a tool to produce high-resolution regional attenuation results. The tests are conducted as a prelude to the regionalization scheme which we will apply to the study of attenuation under Eurasia.

2.2 The Source Pair/Receiver Pair Method

We denote by $A_{i,j}$ the narrow-band filtered time-domain L_g amplitude due to i^{th} source and recorded at the jth station. Inserting instrument amplification I_j, site amplification S_j and source radiation pattern R_i, we parameterize $A_{i,j}$ as

$$A_{i,j} = A_i R_i I_j S_j d_{i,j}^{-1/3} (sin\Delta_{i,j})^{-1/2} e^{\gamma d_{i,j}}, \tag{1}$$

where A_i is the source excitation, $d_{i,j}$ the epicentral distance in kilometers between the ith source and j^{th} station, and Δ the same epicentral distance in degrees. The geometrical spreading coefficient used here follows Nuttli (1973). γ is the coefficient of anelastic attenuation, and is related to the quality factor $Q(f)$ as

$$\gamma(f) = \frac{\pi f}{UQ(f)}, \tag{2}$$

where U is the group velocity.

In RTSM (Chun et al., 1987; Zhu et al. 1991), the pairs of sources and stations are along a great-circle path as shown by the solid lines in Figure 1. It can be readily shown that
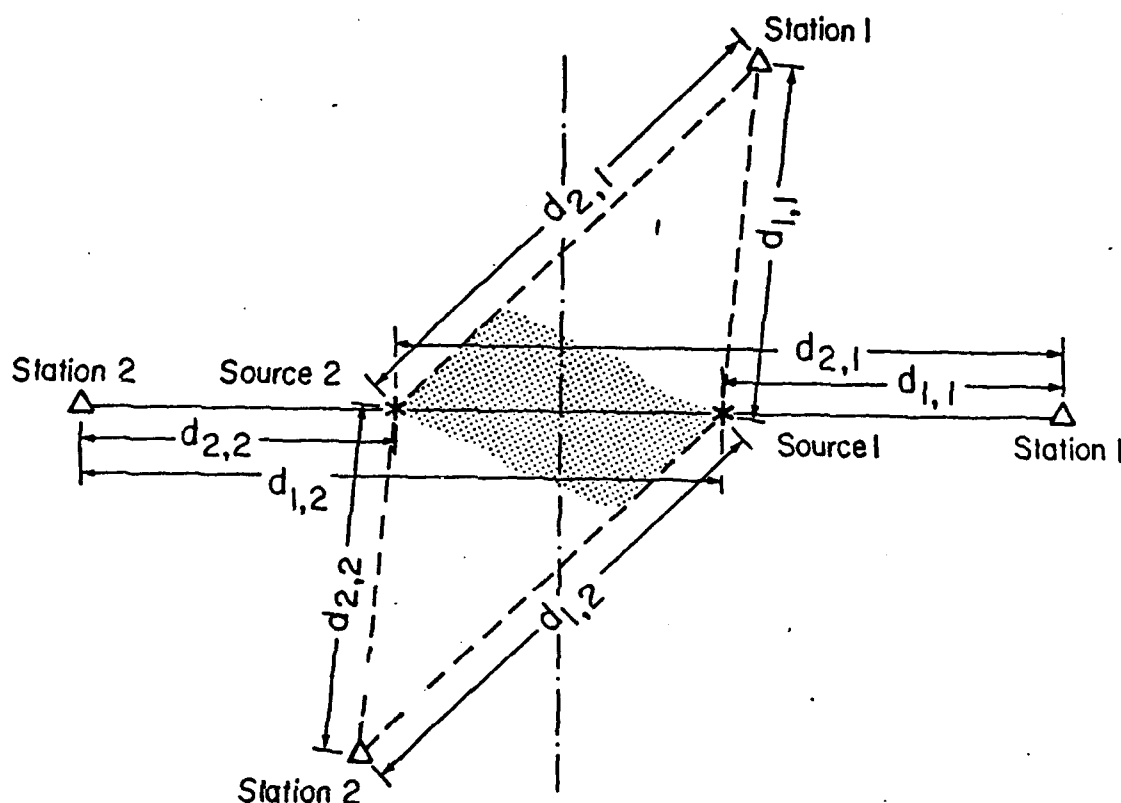
Figure 1. Schematic drawing illustrating the source pair/receiver pair (SPRP) method for measuring L_g attenuation. Solid horizontal lines show an ideal great-circle alignment; dashed lines show the configuration when we relaxed the geometric restriction. The result of the calculation thus describes the attenuation in an area (shaded).

$$\begin{bmatrix} \dfrac{A_{2,1}}{A_{1,1}} & \dfrac{A_{1,2}}{A_{2,2}} \end{bmatrix} \begin{bmatrix} \dfrac{d_{2,1}}{d_{1,1}} & \dfrac{d_{1,2}}{d_{2,2}} \end{bmatrix}^{1/3} \begin{bmatrix} \dfrac{\sin\Delta_{2,1}}{\sin\Delta_{1,1}} & \dfrac{\sin\Delta_{1,2}}{\sin\Delta_{2,2}} \end{bmatrix}^{1/2} = e^{-\gamma(D_1+D_2)}, \tag{3}$$

where $D_1 = d_{2,1} - d_{1,1}$ and $D_2 = d_{1,2} - d_{2,2}$. Note that all source excitation and radiation pattern terms are canceled when the product of the amplitude ratios is taken.

We now assume that the source radiation pattern is azimuthally independent for the regional phases (e.g., Sereno, 1990; Bennett et al., 1990). For L_g phases, the assumption is justified by the fact that the observed L_g phase is actually the superposition of wave propagation in many modes, which tends to smooth out the azimuthal character of the source radiation. Under this assumption, the sources and receivers are no longer required to be co-linear, and the geometrical restriction is relaxed as shown by the dashed lines in Figure 1. We call this generalized version the source pair/receiver pair (SPRP) method.

2.3 L_g Wave Attenuation in Eurasia

For the L_g wave study in time domain, we use the ray paths from 22 selected earthquakes to all 12 CDSN/IRIS stations, including AAK and TLY (Table 1, Table 2 and Figure 2). Data were recorded by broadband instruments at a 20 points/s sampling rate. These events were mostly from crustal depths (Table 1), and thus generated good L_g phase at epicental distances ranging from a few hundreds to more than 5000 kilometers (Figure 3).

The maximum amplitudes of the L_g phases in a series of specific narrow frequency bands are used in time domain analysis. The maximum amplitude (zero to peak/trough) of an L_g phase was measured in the group velocity window from 2.9 to 3.6 km/s (Figure 3). A 4-pole Butterworth bandpass filter was used, and the bandwidth is half of the center frequency, e.g., if the center frequency is 0.5 Hz the filter bandwidth is 0.375 - 0.625 Hz. Following Chun and Zhu (1992), we first take the spectral ratio of the source and receiver pairs. If we let the left-hand side of Equation (3) be Y and take the logarithm on both sides, we have

$$\log Y = -\gamma \Delta D \log e, \tag{4}$$

where ΔD is $D_1 + D_2$ in Equation (3). $\log Y$ is a quantity proportional to γ, and is used as the input of the least-squares fits (Figure 4). We found that the best results from the time domain analysis lie in the frequency range from 0.1 to 1 Hz. This range approximately coincides with that (1-6 sec) found in the description of L_g wave given by Ewing et al. (1957). However, it is lower than the 0.5-2.5 Hz range investigated in detail in a recent study of L_g wave attenuation in eastern Kazakhstan (Sereno, 1990). The scatter of the fits (standard deviation of B) at each centre frequency is at least an order smaller than γ (Figure 4). In general, the variation of $\log Y$ with ΔD in each frequency band is quite linear to at least 4000 kilometers. Based on its value obtained from each narrow-band evaluation, the results of linear regression show that γ is proportional to $f^{0.51}$ (Figure 5). The quality factor at 1 Hz (Q_0) is equal to 564 when the group velocity is taken to be 3.5 km/s.

γ, Q, and their frequency dependence thus derived provide information about L_g attenuation in Eurasia. The exponent of the frequency dependence, 0.51, is in the range spanned by 0.4 of Given et al. (1990) and 0.2-0.7 of Pan et al. (1992), as determined from the L_g and its coda

Table 1. Earthquakes Used in L_g Wave Attenuation Study in Eurasia

Event No.	Date	Origin Time (Hr:Min:Sec)	Latitude (°N)	Longitude (°E)	Depth (km)	Magnitude (mb)
1	15 Apr 1989	20:34:09	29.99	99.20	13	6.2
2	20 Apr 1989	22:59:54	57.17	121.98	26	6.1
3	03 May 1989	05:53:01	30.09	99.48	14	6.1
4	03 May 1989	15:41:31	30.05	99.50	8	5.8
5	17 May 1989	05:04:36	57.09	122.02	31	5.6
6	22 Sep 1989	02:25:51	31.58	102.43	15	6.1
7	30 Sep 1989	18:19:23	23.24	98.85	13	5.3
8	14 Jan 1990	03:03:19	37.82	91.97	12	6.1
9	05 Mar 1990	20:47:01	36.91	73.02	12	5.8
10	26 Apr 1990	09:37:45	36.24	100.25	10	6.3
11	15 May 1990	22:29:59	36.11	100.12	14	5.5
12	14 Jun 1990	12:47:29	47.87	85.07	58	6.1
13	12 Nov 1990	12:28:52	42.96	78.07	19	5.9
14	25 Dec 1990	03:56:46	33.33	75.71	51	5.3
15	05 Jan 1991	14:57:12	23.61	95.90	20	6.2
16	25 Feb 1991	14:30:28	40.39	78.96	21	5.5
17	18 Apr 1991	09:18:31	37.45	68.33	21	5.5
18	26 Apr 1991	22:24:04	38.96	71.05	33	5.4
19	19 Aug 1991	06:05:51	46.94	85.30	30	5.5
20	02 Sep 1991	11:05:50	37.44	95.40	10	5.5
21	12 Sep 1991	00:33:31	54.91	111.11	25	5.1
22	14 Sep 1991	13:16:40	40.17	105.05	25	5.1

Table 2. IRIS/CDSN Station Co-ordinates

Station	Latitude (°N)	Longitude (°E)	Elevation (m)
WMQ (CDSN)	43.821	87.695	970
LZH (CDSN)	36.087	103.840	1560
HIA (CDSN)	49.267	119.740	610
BJI (CDSN)	40.040	116.175	43
MDJ (CDSN)	44.621	129.590	500
KMI (CDSN)	25.123	102.740	1945
OBN (IRIS)	55.100	36.600	130
ARU (IRIS)	56.400	58.600	250
KIV (IRIS)	43.950	42.680	1206
GAR (IRIS)	39.000	70.320	1300
AAK (IRIS)	42.639	72.494	1645
TLY (IRIS)	51.681	103.644	579

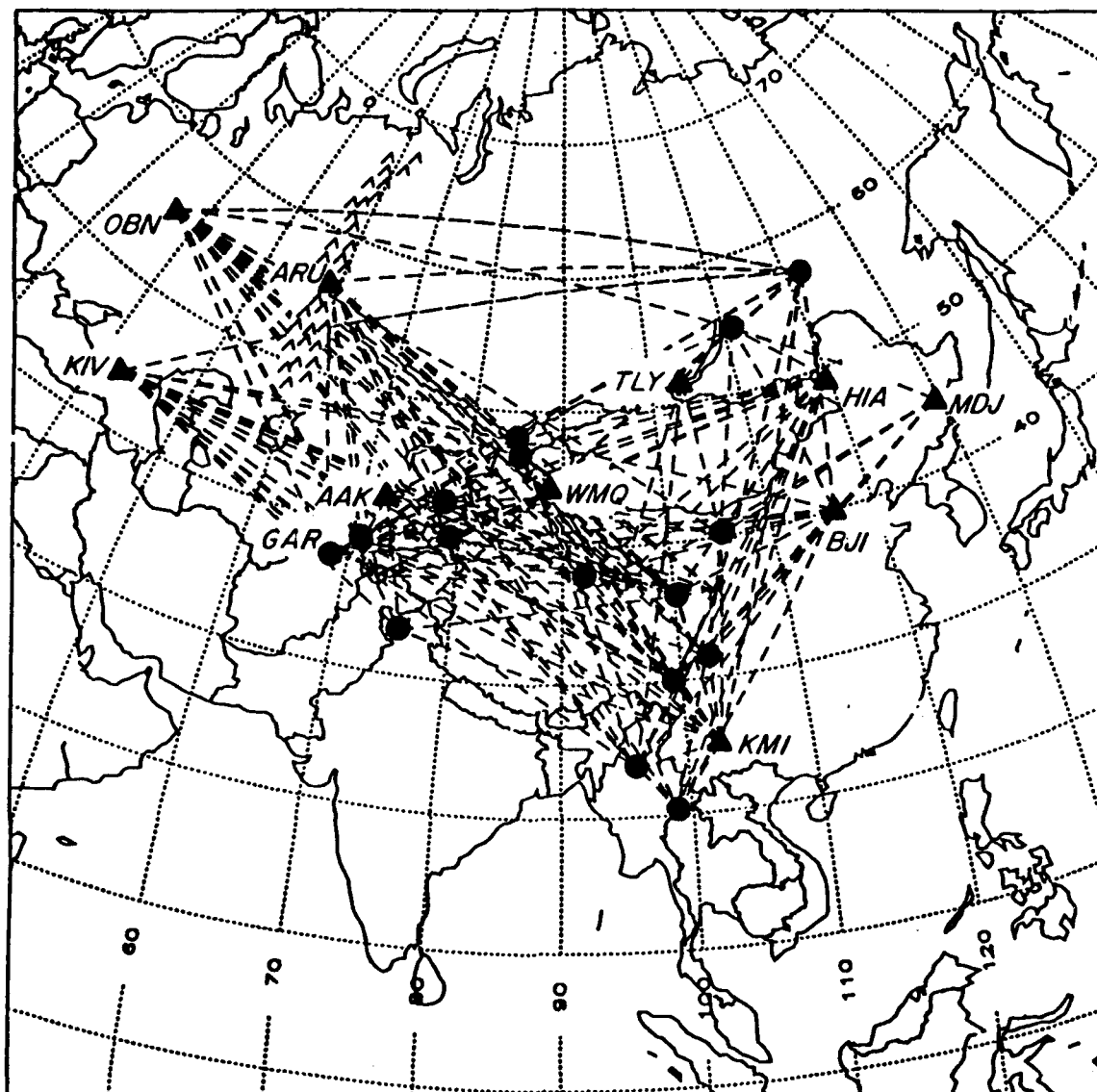* Based on information provided by the Center for Seismic Studies

Figure 2. Map of Eurasia showing the locations of the 22 selected earthquakes (circle) (Table 1), the IRIS/CDSN stations (triangle) (Table 2), and the great-circle paths linking the earthquakes and the stations.
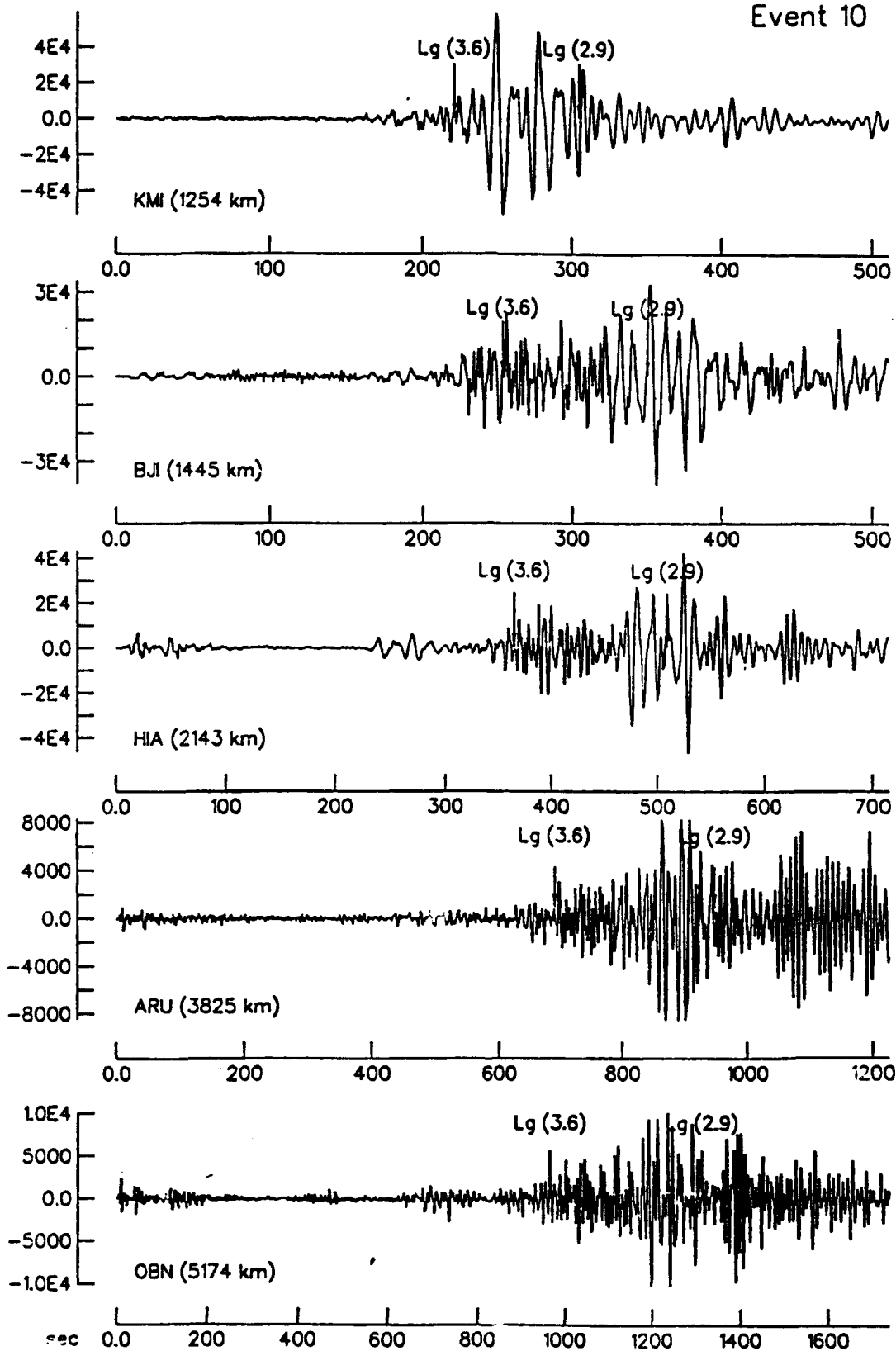
Figure 3. Vertical-component seismograms from CDSN (KMI, BJI, and HIA) and IRIS (ARU and OBN) stations. L_g maxima are measured in a group velocity window from 2.9 to 3.6 km/sec, marked on each trace. The number in the parenthesis following a station name is the epicentral distance.
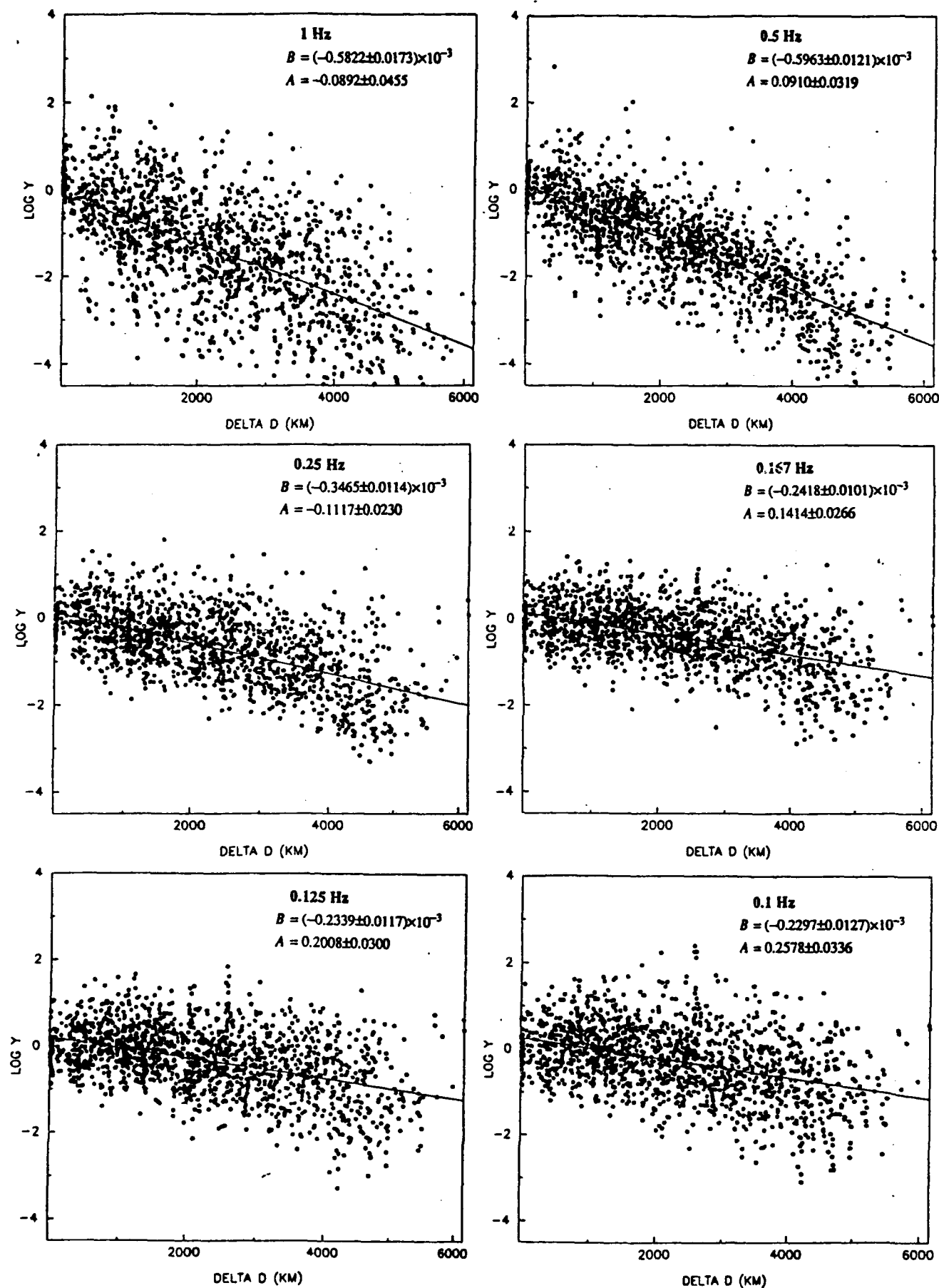
Figure 4. Plots of log$y$ versus ΔD at 1, 0.5, 0.25, 0.167, 0.125 and 0.1 Hz. B is the slope (γlog$e$) and A is the intercept, which should be close to 0.
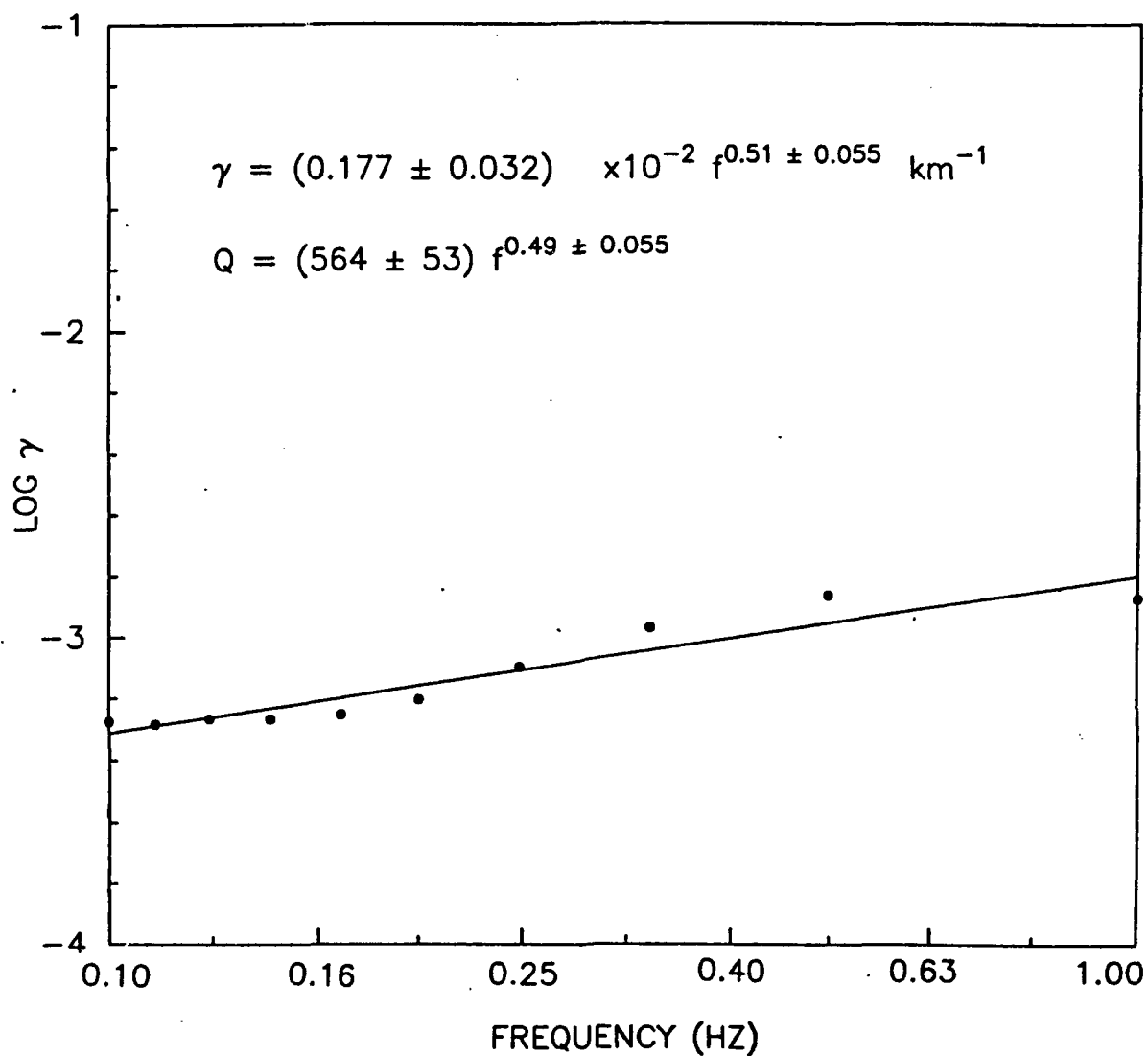
Figure 5. Plot of $\log\gamma$ versus frequency in log scale for L_g wave analysis. γ values are derived from results of the least-squares fits in narrow frequency bands with centre frequencies from 0.1 to 1 Hz.

waves. The Q_0 value is intermediate between 206 for the Great Basin (Chavez and Priestley, 1987) and 1,100 for the Canadian Shield (Chun et al., 1987). This result is also intermediate in the range of Q_0, from 428 to 761, at some IRIS/CDSN stations obtained from the time-domain analysis of L_g phases in regional distances (Bennett et al., 1990). We find that Q with the frequency dependence coefficient $f^{0.51}$ is 396 at 0.5 Hz, compared to the value of 398 at the same frequency, which we obtained from ten events in the region in the previous study (Chun and Zhu, 1992).

2.4 L_g Wave Attenuation under Selected CDSN Station Pairs

To carry out a preliminary regionalization of the L_g wave attenuation in a given subregion, we analyzed selected ray paths confined mostly within it. In practice, it translated into using only short (< 2000 km) L_g paths.

Data from two station pairs, LZH-KMI (LK) and LZH-WMQ (LW), turned out to have enough events (12 and 14, respectively) and combinations (45 and 40, respectively) to calculate the frequency-dependent attenuation coefficient (γ) by a least-squares fit (Figure 6). As before, we used narrow-band filtering and time-domain amplitude measurement. Figure 7 shows the frequency-dependent attenuation for the regions traversed by the ray paths from the events to the stations. We found that the frequency dependence in the individual regions ($f^{0.42}$ and $f^{0.45}$ for LK and LW, respectively) is similar to the average value ($f^{0.49}$) obtained for Eurasia. Q_0 obtained from the LK inter-station paths, which has a substantial segment lying between the Tibetan Plateau and the interior paraplatforms, is 485. This value is slightly higher than the Q_0 of L_g (400 and 450) in Jianchuan, Yunan province (Wu et al., 1987), and much higher than the Q_0 (312 - 380) obtained by Nuttli (1986) for paths between the Shagan River test site in the former USSR and the WWSSN stations south of the Tibetan Plateau. The Q_0 obtained from the LW inter-station paths is 519, indicating less attenuation in the paraplatforms northeast of the Tibetan Plateau, away from the active tectonics. The value is approximately equal to the mean value between the Q_0 of the northwestern and southwestern China (599 and 445, respectively), determined from L_g studies of short-period analog recordings (Chen and Nuttli, 1984). However, Q_0 in these two regions are lower than the value obtained for the entire Eurasia, indicating that the L_g attenuation is probably high in the south and low in the north in Eurasia as suggested by Pan et al. (1992).
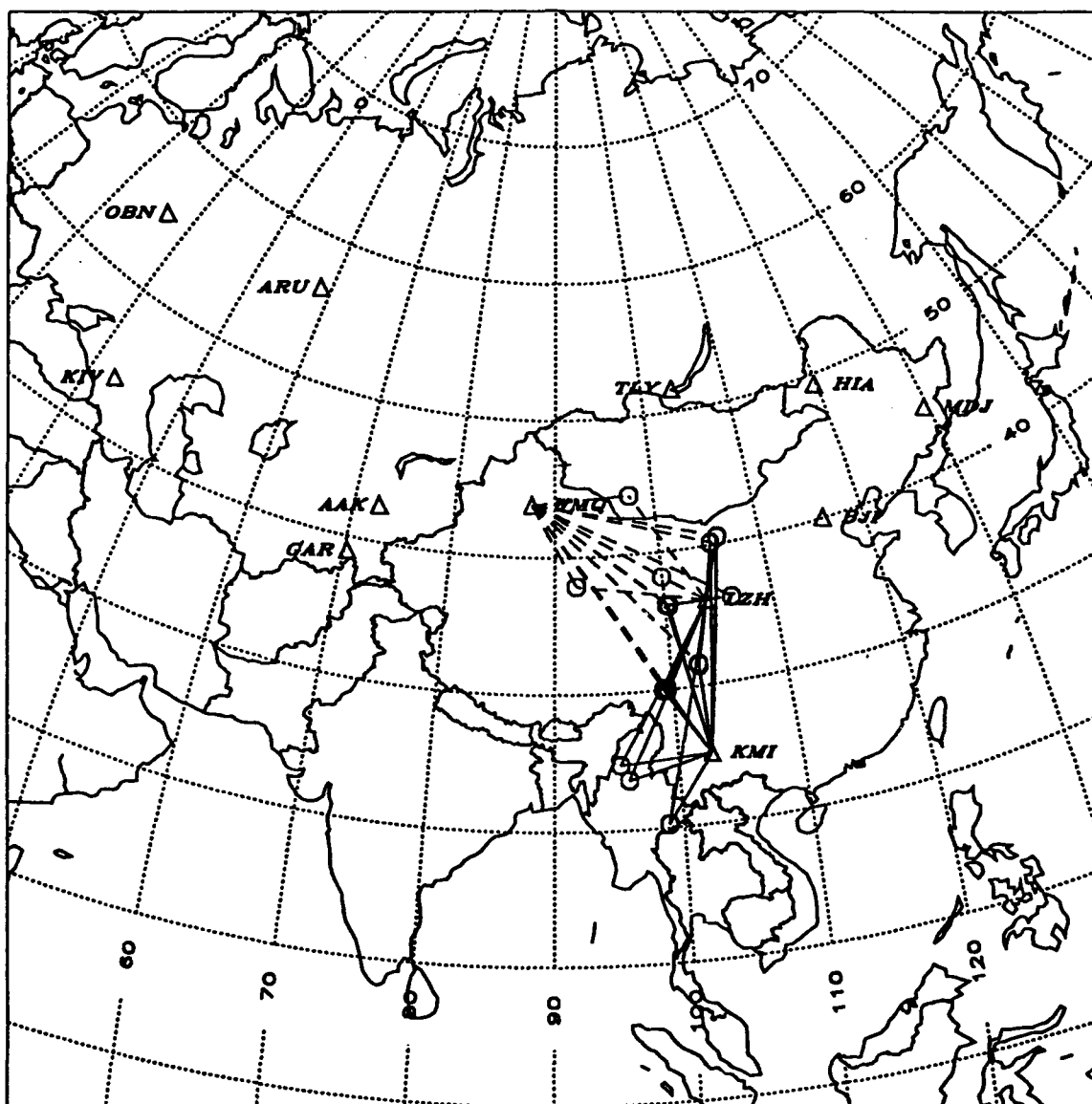
Figure 6. Map showing great-circle paths from the earthquakes (circle) to the LK and LW station pairs (triangle) for the preliminary regionalization of L_g wave attenuation.
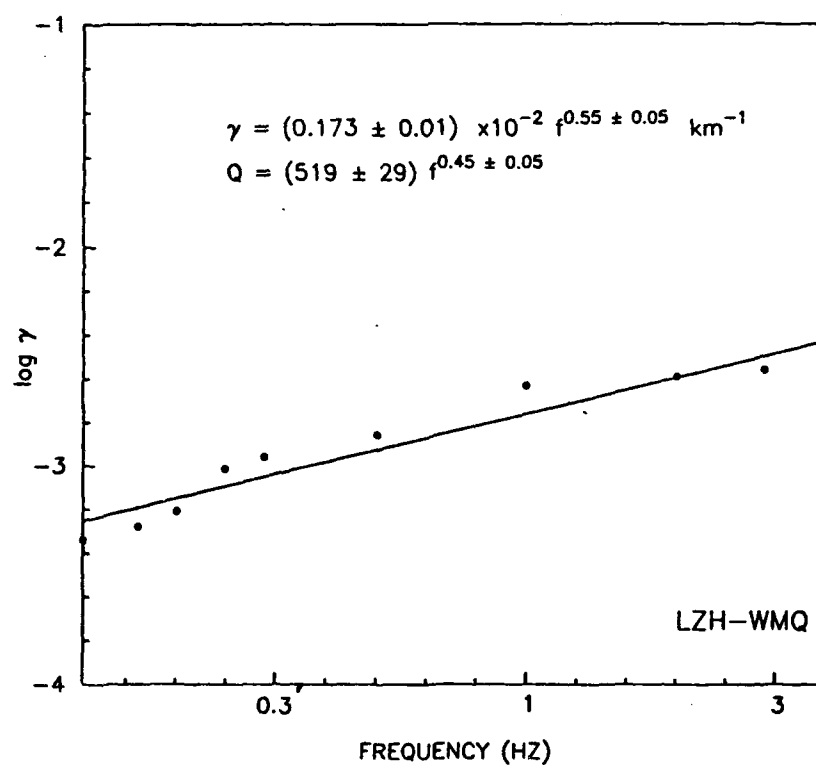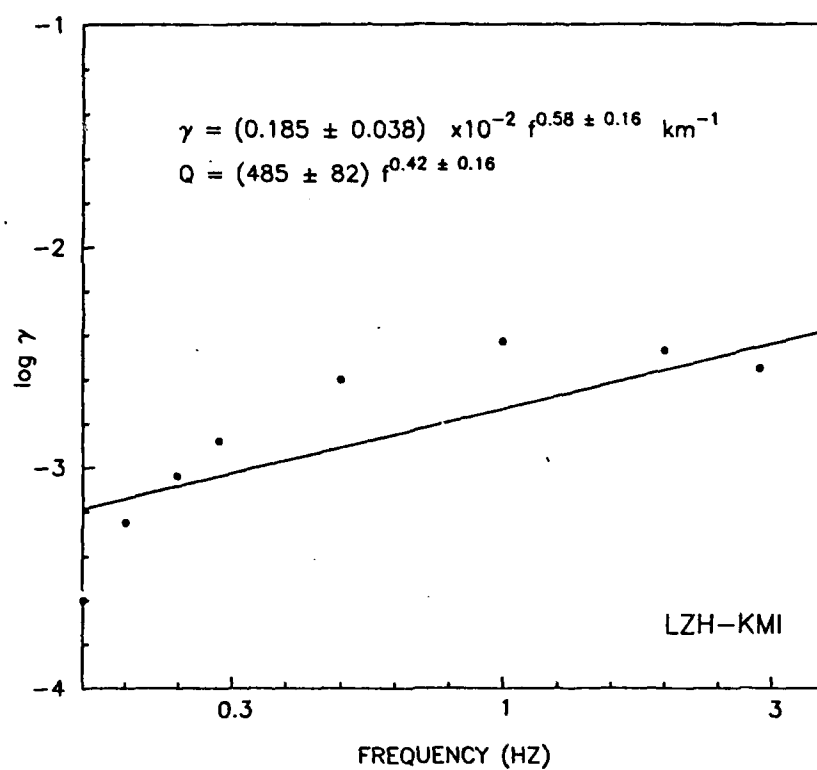
$$\gamma = (0.185 \pm 0.038) \times 10^{-2} \, f^{0.58 \pm 0.16} \, \text{km}^{-1}$$
$$Q = (485 \pm 82) \, f^{0.42 \pm 0.16}$$

LZH−KMI

FREQUENCY (HZ)

$$\gamma = (0.173 \pm 0.01) \times 10^{-2} \, f^{0.55 \pm 0.05} \, \text{km}^{-1}$$
$$Q = (519 \pm 29) \, f^{0.45 \pm 0.05}$$

LZH−WMQ

FREQUENCY (HZ)

Figure 7. Results of L_g attenuation along the inter-station paths of stations LZH and KMI (top), and stations LZH and WMQ (bottom).

III. PRELIMINARY ANALYSIS OF L_g WAVE
ATTENUATION UNDER BEIJING TELEMETERED NETWORK (BTN)

3.1 Introduction

The Beijing Telemetered Network (BTN) consists of 29 vertical-component stations (Figure 8), of which station BJ in Beijing collocates with the CDSN station BJI. Two types of seismometers, DS-1 and 768, are deployed at BTN stations, both having flat displacement response between 0.1 and 10 Hz. The station calibrations are conducted daily. The time code uses Beijing time and is corrected every two hours with respect to the time signals broadcasted by Shanxi Astronomical Observatory. The system operates in triggered mode, the pretrigger time being 30.72 sec. Data are digitized at 100 points/sec.

   With numerous stations and events, we have tested and developed means, based on the reversed two-station method (RTSM, Chun et al., 1987), to analyze data collected at sparsely-located permanent stations. We here introduce an extended RTSM method, in which we first calculate the spectral ratio of seismograms at two stations from one event to cancel the source effects, and then calculate the spectral ratio of a three-event combination to cancel the site effects (Figure 9). The method is applied to the L_g wave attenuation study in an area traversed by the ray paths from 13 local and regional earthquakes to the stations of BTN.

3.2 The Extended Reversed Two Station Method

We denote by F the spectral amplitude of the L_g wave. F can be expressed in the form

$$F_{i,j}(f,d) = S_i(f)R_i(f,\theta)G_{i,j}(d)\Gamma_{i,j}(f,d)I_j(f)SS_j(f) \tag{5}$$

where f denotes the frequency, d the epicentral distance, θ the station azimuth. $F_{i,j}$ represents the L_g spectral amplitude due to the ith source and recorded at the jth station. The parameters on the right-hand side of the equation include the source excitation function (S), source radiation pattern (R), geometrical spreading function ($G = d^{-0.5}$), instrument response (I), station site response (SS), and the anelastic attenuation function, which can be written as

$$\Gamma(f,d) = e^{-\gamma d}. \tag{6}$$

The coefficient is related to the quality factor $Q(f)$ by Equation (2).

   Consider the diagram in Figure 9 where stations 1 and 2 are aligned with event 1 along a great-circle path, the spectral ratio taken at this stage cancels the source terms (S and R). When event 2 is not along the great-circle path with stations 1 and 2 and therefore, a perfect two-station reversal is impossible, we add in station 3 and event 3. If a station-event pair is found to be nearby each apex of the triangular configuration (solid lines in Figure 9), we have the following equation after cancellation of the site response term (SS) and the instrument response (I):
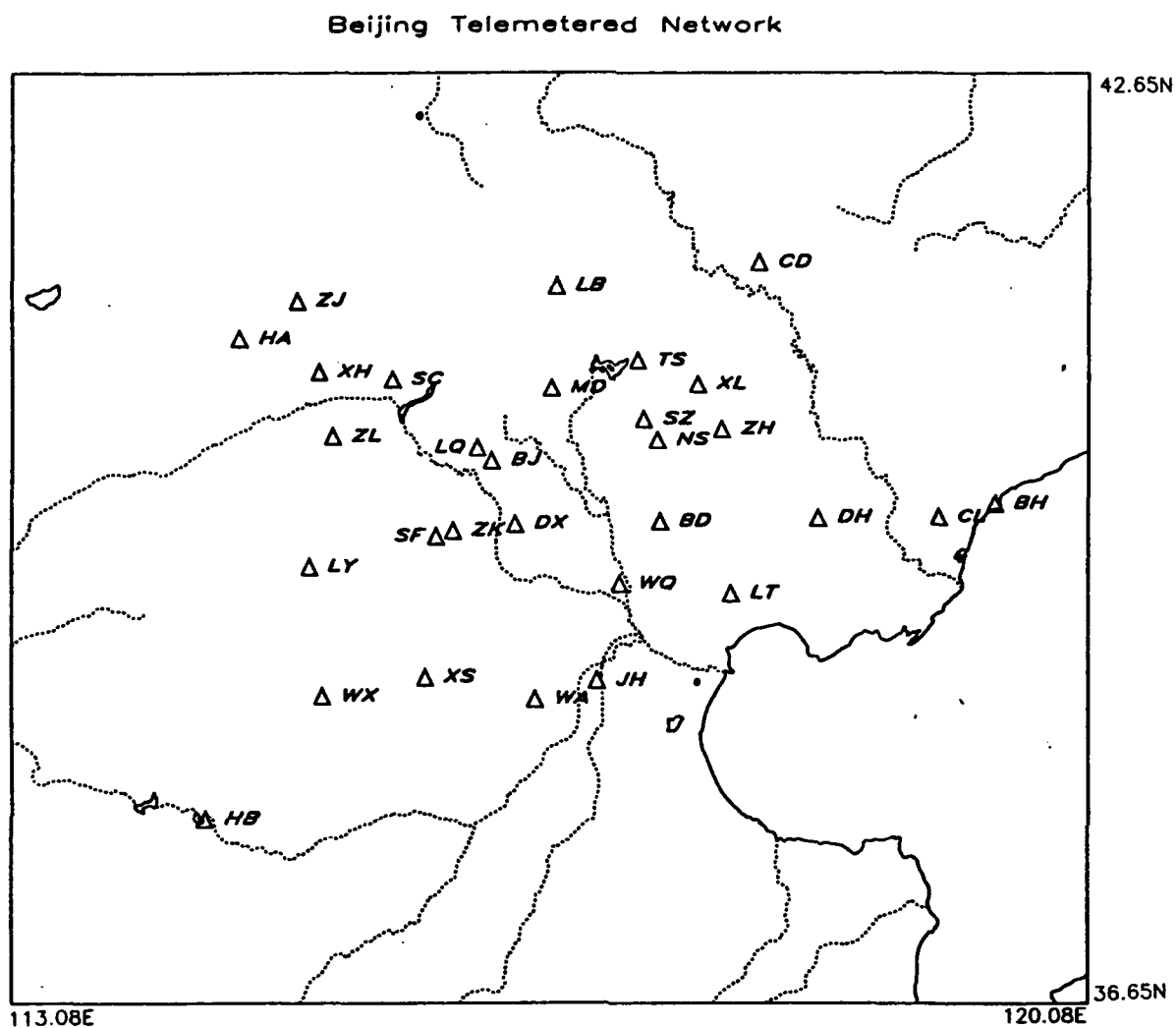
Beijing Telemetered Network

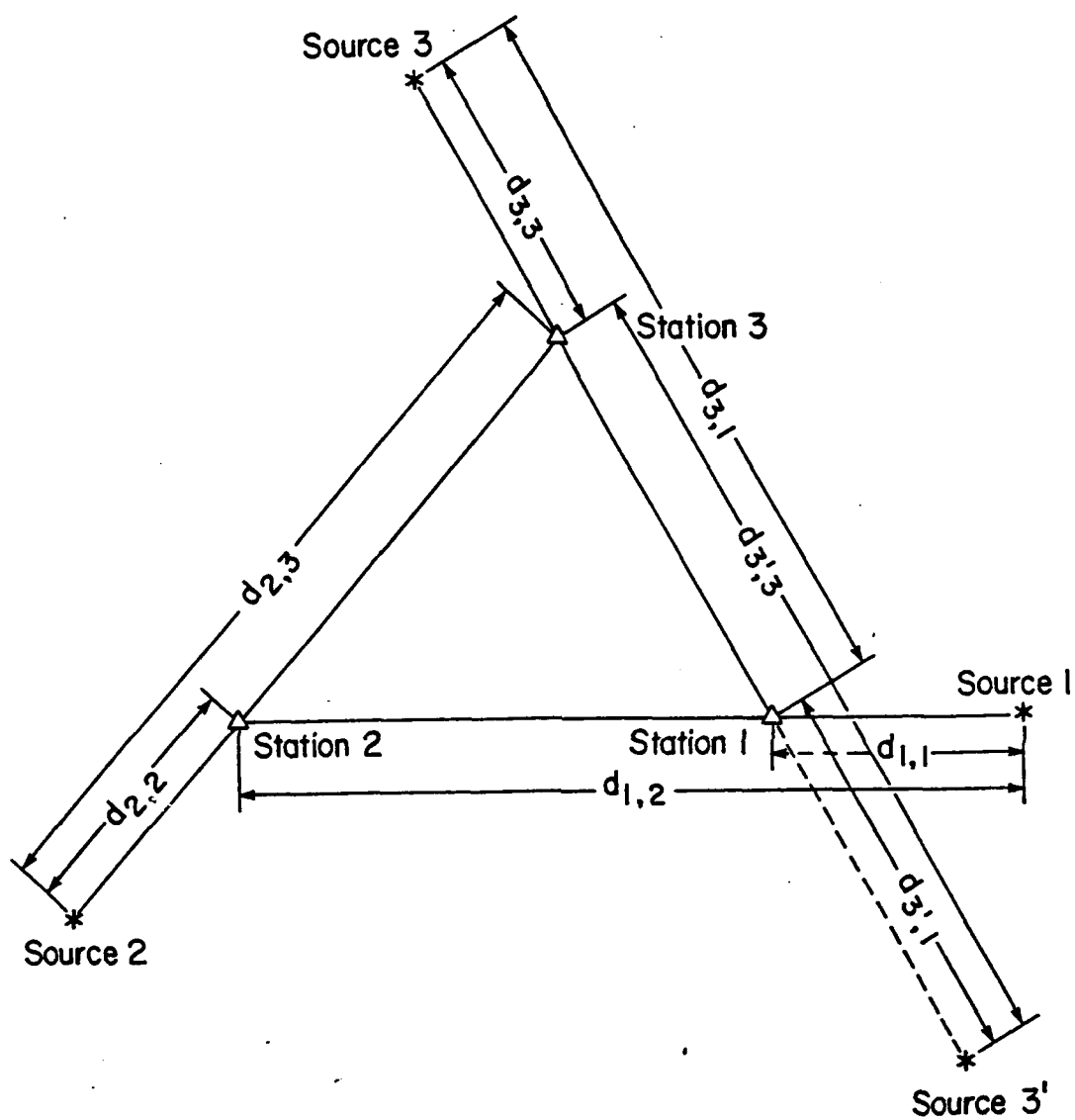Figure 8. Station locations of the Beijing Telemetered Network (BTN).

Figure 9. Schematic drawing illustrating the configuration of the extended reversed two-station method. Solid lines represent a normal station-event combination in which each apex of the triangle has a station and an event; dashed lines represent a combination in which two events are associated with one apex of the triangle (Station 1) to accommodate the absence of an event at the other apex (Station 3) (see text).

$$\left[\frac{F_{1,2}\ F_{2,3}\ F_{3,1}}{F_{1,1}\ F_{2,2}\ F_{3,3}}\right]\left[\frac{d_{1,2}\ d_{2,3}\ d_{3,1}}{d_{1,1}\ d_{2,2}\ d_{3,3}}\right]^{0.5}=e^{-\gamma(D_1+D_2+D_3)}\ . \tag{7}$$

where $D_1 = d_{1,2} - d_{1,1}$, $D_2 = d_{2,3} - d_{2,2}$, and $D_3 = d_{3,1} - d_{3,3}$. On the other hand, if there is no event close to a station at one of the apexes, we may use two events close to the station at another apex (dashed line in Figure 9) to form a combination, and we then have

$$\left[\frac{F_{2,3}\ F_{1,2}\ F_{3',1}}{F_{2,2}\ F_{1,1}\ F_{3',3}}\right]\left[\frac{d_{2,3}\ d_{1,2}\ d_{3',1}}{d_{2,2}\ d_{1,1}\ d_{3',3}}\right]^{0.5}=e^{-\gamma(D_1+D_2-D'_3)}\ . \tag{8}$$

where $D_1 = d_{1,2} - d_{1,1}$, $D_2 = d_{2,3} - d_{2,2}$, and $D_3 = d_{3',3} - d_{3',1}$. At this stage, the left-hand side of the equation is a constant, logarithmically proportional to γ. We call it the extended reversed two-station method (extended RTSM).

3.3 Preliminary Result of L_g Wave Attenuation

A total of 13 local and regional events (Table 3 and Figure 10) were used to test the extended RTSM method. All of them were of crustal depths. The 46 seismograms from ten of the BTN stations (Table 4) resulted in nine triangles (inset of Figure 10) and 42 possible combinations. Data used in this preliminary analysis had been reprocessed in China prior to being shipped to us. We found that they are of two different sampling rates, 12.5 points/s and 50 points/s. We re-sampled the data at 25 points/s before any calculation, and the spectra are considered meaningful up to 6 Hz. At epicentral distances ranging from 100 to 1000 kilometers, L_g waves at most of the stations appear to be the most prominent phase, stronger than the first P arrivals (Figure 11). Power spectra (Figure 12) of these seismograms show that the energy of the L_g waves usually peaks around 1 Hz, more stable than respective P arrivals and has magnitude several orders greater than the noise proceeding the P arrival.

Spectra of the L_g waves were calculated in a group-velocity window from approximately 3.0 to 3.5 km/s, i.e., the beginning of the window was sometimes shifted to include the first motion of an L_g phase. After reduction, the spectra (γ) of all combinations were stacked. The least-squares regression of the averaged spectra ratio in Figure 13 shows the frequency dependence of γ. In frequency range of 0.3 - 6 Hz, the attenuation coefficient

$$\gamma = (0.317 \pm 0.006) \times 10^{-2} f^{0.28 \pm 0.016}\ km^{-1}\ . \tag{9}$$

The above equation gives a γ of 0.00350 km^{-1} at 1.43 Hz, comparable to the γ (0.0034 km^{-1}) at the same frequency published in the map of L_g wave attenuation in continental China (Jiang and Ge, 1989). The latter also shows that γ decreases westward (0.002 km^{-1}) and northward (0.0027 km^{-1}). The Q_0 is thus 283, based on a group velocity of 3.5 km/s. The value is much lower than Q_0, e.g., 550 (Wu et al., 1987) and 403 (Chen and Nuttli, 1984), determined in time-domain. Compared to our general and regional studies in Eurasia, the low Q and its high frequency dependency suggest that attenuation in the area under investigation is probably at the high end of the entire Eurasia except the active tectonic region in central Asia. However, the consistency between the time and frequency domain results is to be investigated.

Table 3. Earthquakes Used in L_g Wave Attenuation Study under BTN

| Event No.	Date	Origin Time (Hr:Min:Sec)	Latitude (°N)	Longitude (°E)	Magnitude (mb)
812302	30 Dec 1988	18:34:29.4	37.60	115.05	2.6
905075	07 May 1989	20:57:20.9	40.27	115.72	4.1
907051	05 Jul 1989	20:48:54.6	37.48	115.02	3.1
911052	05 Nov 1989	10:28:46.7	40.08	118.17	3.3
801012	01 Jan 1988	23:25:09.9	43.35	111.25	3.8
003132	15 Feb 1990	03:21:14.7	39.70	118.65	3.0
002272	27 Feb 1990	03:21:06.3	41.83	120.75	4.3
003082	08 Mar 1990	08:11:47.7	40.95	106.83	4.8
003121	12 Mar 1990	15:59:30.0	37.20	113.88	4.3
004153	15 Apr 1990	20:37:06.0	42.70	117.30	4.6
004202	20 Apr 1990	05:52:34.0	39.75	118.40	4.7
004211	21 Apr 1990	06:07:40.3	39.78	118.72	3.5
012151	15 Dec 1990	03:27:18.5	36.77	114.90	3.4
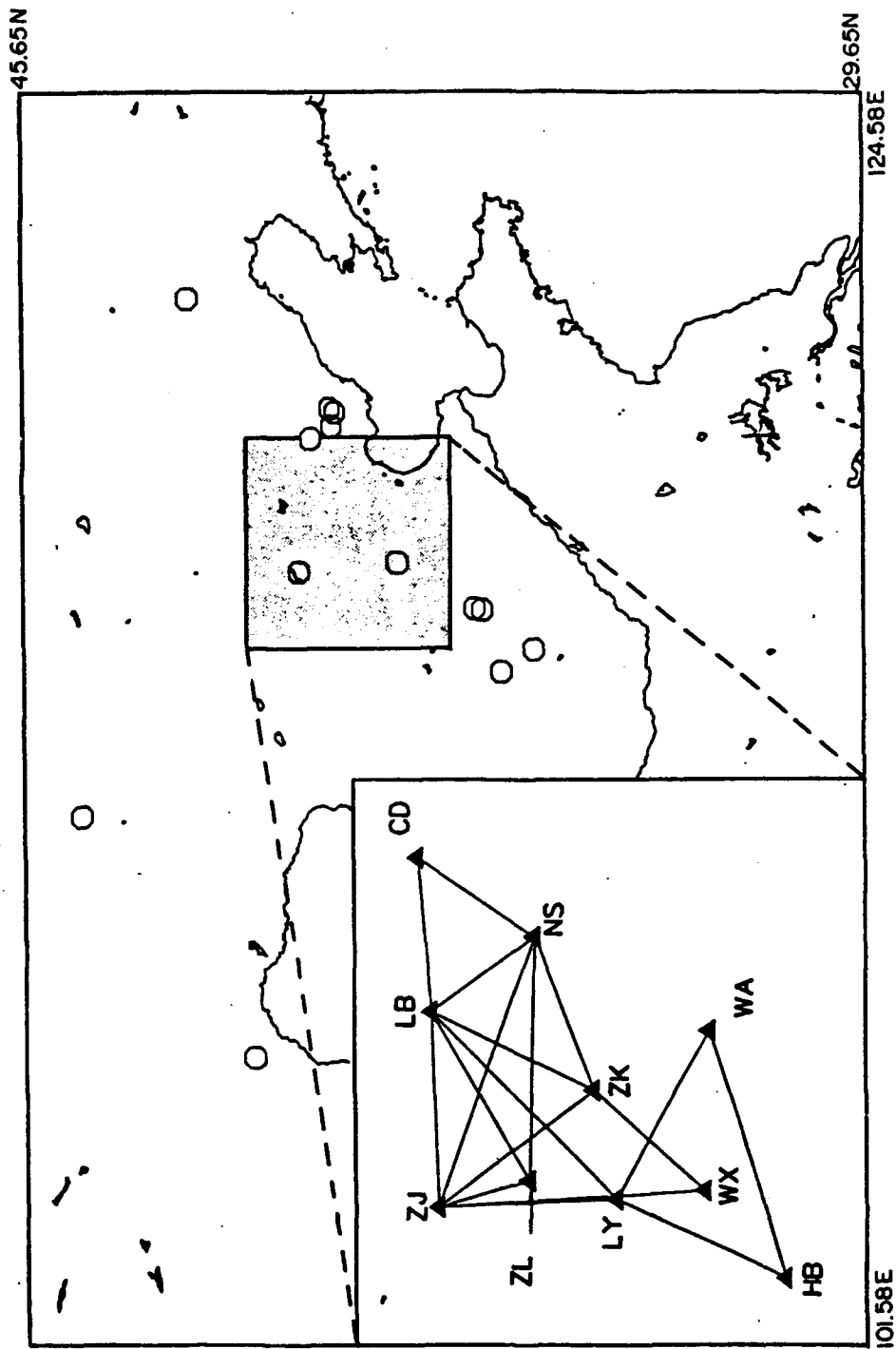
Figure 10. Map of Northern China showing the locations of the 13 selected earthquakes (Table 3). Inset: nine 3-station combinations used in the L_g wave attenuation analysis.

Table 4. Co-ordinates of the BTN Stations in Figure 10

Station	Latitude (°N)	Longitude (°E)	Elevation (m)
CD	41.015	117.916	400
HB	38.248	114.307	140
LB	40.900	116.596	510
LY	39.510	114.980	880
NS	40.140	117.253	100
WA	38.847	116.454	-266
WX	38.864	115.063	100
ZJ	40.829	114.900	835
ZK	39.688	115.923	120
ZL	40.157	115.133	1100

* Based on Quaterly Earthquake Report of Beijing Telemetered Network (1990) published by the Chinese Seismological Bureau.
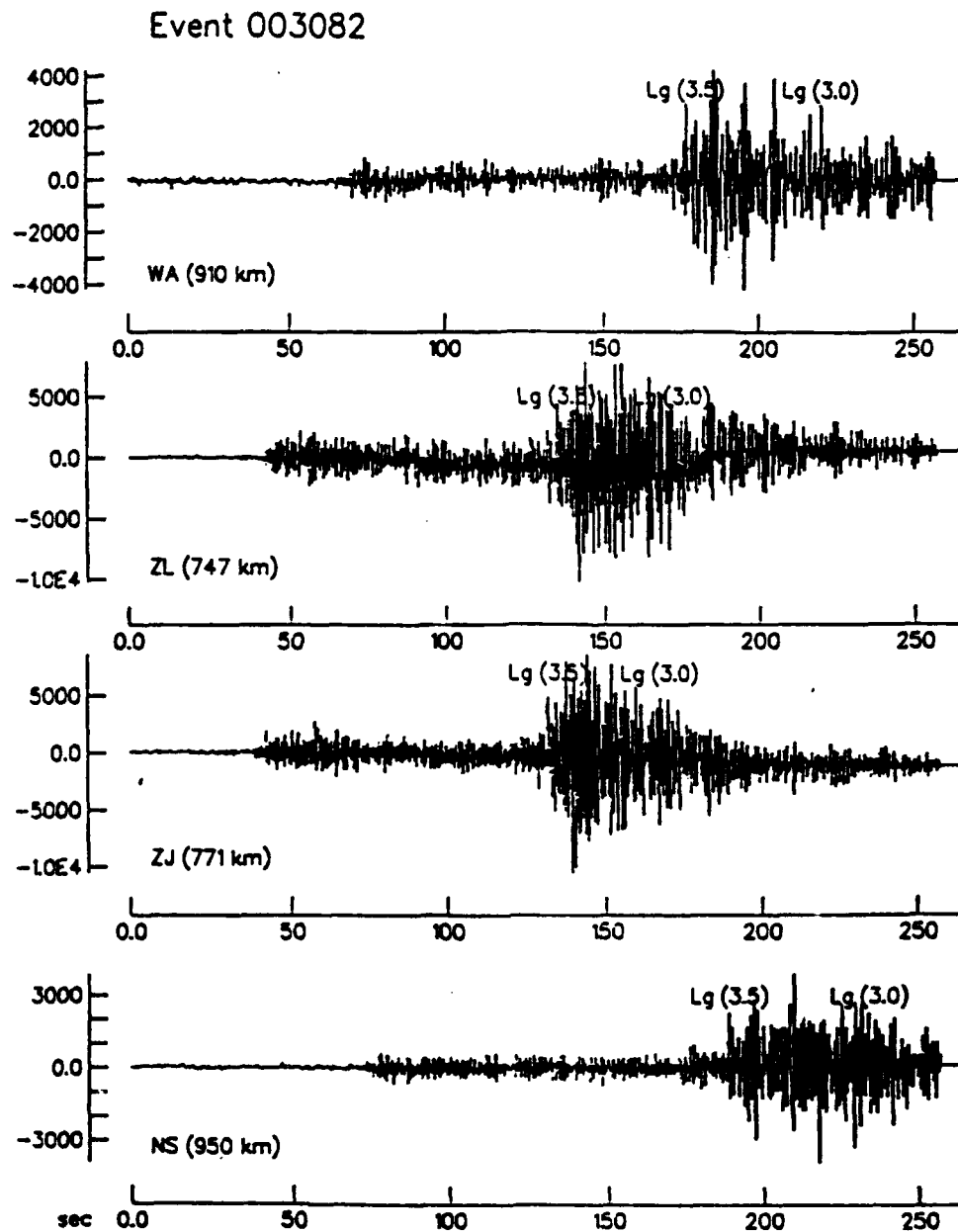
Figure 11. Vertical seismograms from BTN used in the L_g wave analysis. An L_g wave in group velocity window from 3.5 to 3.0 km/sec is used for spectral calculation. The number in the parenthesis following a station name is the epicentral distance.
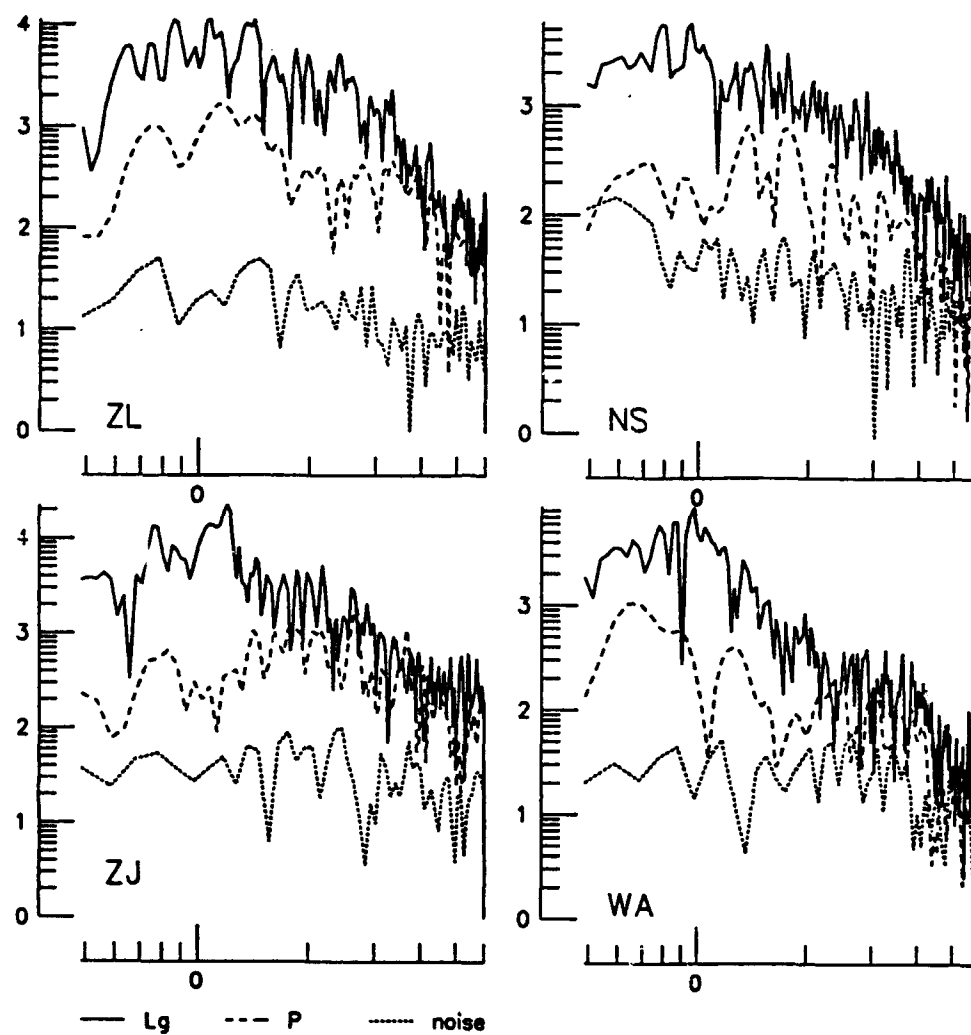
Figure 12. Spectra of the seismograms in Figure 11 showing relative energy distribution of the P, L_g, and the noise preceding the P arrival.
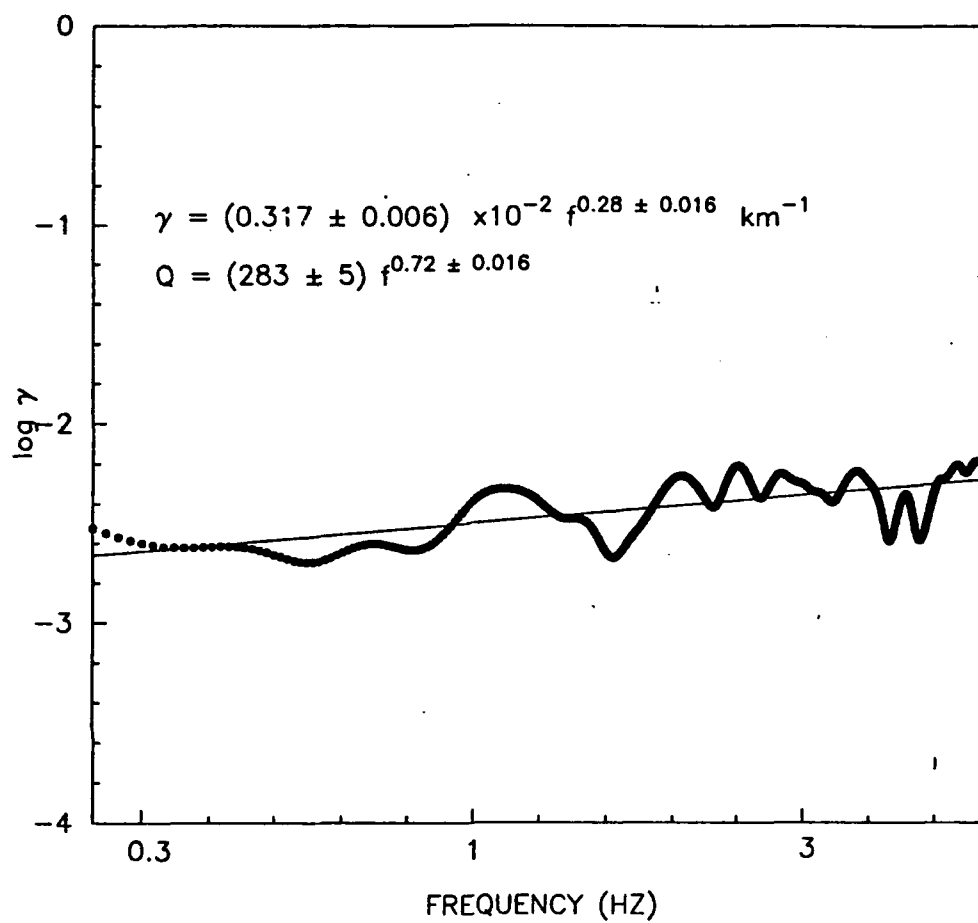
Figure 13. Plot of averaged spectral ratios and the result of least-squares regression of the attenuation coefficient of the L_g waves.

IV. DISCUSSION AND CONCLUSIONS

4.1 Summary of the Research Program

The research described here represents the first-year effort of our two-year project designed to develop methodology for site and source corrected attenuation measurement and to study the frequency-dependent attenuation in Eurasia. Our research has been focused on methodology extended from the RTSM, and their application has brought a general evaluation of the frequency dependent attenuation in Eurasia.

The key difference between the two new methods, i.e., the SPRP method and the extended RTSM, and the RTSM is that the results from the new methods represent the attenuation of an area enclosed by the stations/events involved in a combination instead of the inter-station (event) path. The SPRP method is characterized by a greater flexibility than the RTSM. It allows attenuation measurements to be made using sparse recordings from a seismic network with only a brief recording history. Results from our study of IRIS/CDSN data indicate that isolating the path effect by taking time-domain amplitude ratios following a much relaxed geometry is justified. The extended RTSM method has shown another possibility of studying regional wave attenuation for cases in which the reversal of the station-event pairing along the great-circle path is impossible. The method is designed for attenuation study of the waves that are affected by the source characteristics. By simultaneous cancellation of the site and source effect, application of either method leads to frequency-dependent attenuation measurements. Further, we have employed configurations of stations straddling the sources in performing the SPRP method and the sources straddling the stations in performing the extended RTSM. With slight algebraic difference, either arrangement serves the purpose of canceling the site and source effects.

We have conducted generalized time-domain analysis of L_g wave attenuation in Eurasia. After a preliminary analysis of a 10-event data set, results from a 22-event data set are consistent with the preliminary study, and have shown that L_g wave attenuation at low frequencies (0.1-1.0 Hz) exhibits greater stability and consistency than its higher-frequency counterpart. Frequency-dependent attenuation measurements (γ, Q_0, and f^n) are intermediate to the values in the different areas in Eurasia suggested by previous studies. Preliminary time-domain analyses in the two subregions of Eurasia have shown that while its frequency dependence varies within the error bounds of the average value determined for the entire Eurasia, the L_g wave attenuation as quantified by the quality factor (Q) may vary considerably across Eurasia. The variation seems to be directly related to the current tectonic activity and various geological components traversed by long ray paths.

4.2 Research Plan for the Second Year

In the second year of the project, our research will focus on developing methodology to regionalize the site and source corrected attenuation measurements for a sparsely-located seismic network such as the IRIS/CDSN stations. Scientifically, we will concentrate on two topics: (1) determination of frequency-dependent attenuation parameters in the subregions of

Eurasia, and (2) investigation of the consistency between the attenuation parameters resulted from time- and frequency-domain analyses.

In our proposed scheme for regionalizing L_g wave attenuation, we divide the study region into rectangular grids, and the γ_i of each rectangle is to be determined in a 2-D least-squares inversion. The input for the inversion is the site/source corrected attenuation measurements by the RTSM and/or SPRP methods, except that the reduction now involves segmented distances along a single ray path because of the grids. With fixed geometrical spreading parameter, the γs will be solved through the least-squares inversion with large number of ray paths. Since the input of the inversion is obtained in a way independent of any source and site effects, we expect that the inversion will lead to the first stable pure-path determination of the attenuation in individual areas of Eurasia, including detailed information of attenuation under BTN.

.We plan to investigate the large discrepancy of Q values between the time- and frequency domain analyses under BTN, and the consistency between the attenuation analyses in time and frequency domains at large, by examining the variation of the attenuation parameters (γ, Q and f^n) when the same site/source correcting procedures are applied to the analyses in different domains. Analyses using IRIS/CDSN data may result in evaluations directly applicable to the attenuation study in Eurasia. However, the dense station distribution and relatively abundant seismic events in the area covered by BTN will provide opportunities for a comparison between the the time- and frequency-domain analyses in local and regional distance ranges. Results from these distance ranges are essential in obtaining accurate measurements in nuclear verification problems.

Achnowledgements

References

Bennett, T. J., J. F. Scheimer, A. K. Campanella, and J. R. Murphy (1990). Regional discrimination research and methodology implementation : Analyses of CDSN and Soviet IRIS data, *S-Cubed Report SSS-TR-90-11757*, Technical Report on Contract No. f19628-89-C-0043.

Chavez, D. E., and K. F. Priestley (1987). Apparent Q of P_g and L_g in the Great Basin, paper presented at the 9th Annual DARPA/AFGL Seismic Research Symposium, June 1987.

Chen, P. S. and O. W. Nuttli (1984). Estimates of magnitudes and short-period wave attenuation of Chinese earthquakes from modified Mercalli Intensity data, *Bull. Seism. Soc. Am.*, 74, 957-968.

Chun, K.-Y., G. F. West, R. J. Kokoski, and C. Samson (1987). A novel technique for measure L_g attenuation - results from Eastern Canada between 1 to 10 Hz, *Bull. Seism. Soc. Am.*, 77, 398-419.

Chun, K.-Y., and T. Zhu (1992). Regional wave attenuation in Eurasia, *Semi-Annual Tech. Rep.*.

Chun, K.-Y., T. Zhu and X. R. Shih (1992). Regional wave attenuation in Eurasia, paper presented at the 14th Annual PL/DARPA Seismic Research Symposium, September 1992.

Ewing, M., W. Jardetzky, and F. Press (1957). *Elastic Waves in Layered Media*. New York: McGraw-Hill.

Given, H. K., N. T. Tarasov, V. Zhuravlev, F. L. Vernon, J. Berger, and I. L. Nersesov (1990). High-frequency seismic observations in eastern Kazakhstan, USSR, with emphasis on chemical explosion experiments, *J. Geophys. Res.*, **95**, 295-307.

Jiang, Y., and H. Ge (1989). Relationships between L_g attenuation and geotectonic characters in China, *Geophysics in China in the Eighties*, 317-324.

Nuttli, O. W. (1973). Seismic wave attenuation and magnitude relations for eastern North America, *J. Geophys. Res.*, **78**, 876-885.

Nuttli, O. W. (1986). L_g magnitudes of selected East Kazakhstan underground explosion, *Bull. Seism. Soc. Am.*, **76**, 1241-1251.

Nuttli, O. W. (1988). L_g magnitudes and yield estimates of Novaya Zemlya nuclear expolosions, *Bull. Seism. Soc. Am.*, **78**, 873-884.

Pan, Y., B. J. Mitchell, and J. Xie (1992). L_g coda Q across Northern Eurasia, paper presented at the 14th Annual PL/DARPA Seismic Research Symposium, September 1992.

Sereno, T. J. (1990). Frequency-dependent attenuation in eastern Kazakhstan and implications for seismic detection thresholds in the Soviet Union, *Bull. Seism. Soc. Am.*, **80**, 2089-2105.

Wu, F., P. Wang, and Y. Chen (1987). Q_P and Q_S in Beijing and Jianchuan of Yunan regions, *ACTA Seismologica Sinica*, **9**. 337-346.

Zhu, T., K.-Y. Chun, and F. W. Gordon (1991). Geometrical spreading and Q of P_n waves: An investigative study in eastern Canada, *Bull. Seism. Soc. Am.*, **81**, 882-896.